Fourth International Meeting on Wind Turbine Noise

Rome Italy 12-14 April 2011

Trailing Edge Noise Reduction of Wind Turbine Airfoils by Active Flow Control

Authors: A. Wolf, Th. Lutz, W. Würz, O. Stalnov*, A. Seifert*
IAG, University of Stuttgart, Germany, wolf@iag.uni-stuttgart.de;
TAVU*, Tel-Aviv University, Israel, stalnov@eng.tau.ac.il

Abstract

Noise is a crucial factor in wind turbine rotor design, as wind turbines move closer to inhabitant regions as the world wide energy consumption further increases. Active Flow Control is expected to be a convenient solution to reduce the trailing edge noise, which is the main source of noise at wind turbines [1], and to increase the performance of the turbine as well. This paper deals with constant suction and shows the impact on various boundary layer parameters, which influence the emitted trailing edge noise. Numerical and experimental results are presented showing that constant suction leads to a significant reduction of trailing edge noise.

Introduction

Wind farms can not be located too close to inhabitant regions due to prohibitive levels of noise emission. The noise emitted from operating wind turbines can be divided into two sources: mechanical, and flow-induced. In this study, we are interested in attenuating flow-induced noise, namely the turbulent boundary layer – trailing edge interaction noise (TBL-TE noise), which is considered to be the most dominant noise source of modern wind turbines [1]. This noise is generated by turbulent pressure fluctuations in the boundary layer, which are scattered at the trailing edge of the turbine blade. Currently noise reduction is achieved by airfoil shape design [2] or other passive devices like serrated trailing edges [3]. A candidate technology for further reducing the noise levels resulting from turbulent structures interacting with the trailing edge is Active Flow Control (AFC). Flow control techniques affect the boundary layer features and as such it can be expected that also the emitted trailing edge noise will be influenced. Currently, numerical and experimental investigations are performed at the University of Stuttgart and Tel-Aviv University to investigate the effect of AFC on the boundary layer and their potential for trailing edge noise reduction.

Numerical Model and Results

Different types of actuation systems were simulated at the IAG. First a single slot device was tested to investigate the general effect of suction on the relevant boundary layer parameters and the emitted trailing edge noise. The latter was determined by the Noise prediction tool Rnoise [4], which was developed at the IAG. It is based on the theory of Blake [5] solving a Poisson equation. For the wall pressure fluctuations caused by the turbulent boundary layer Blake showed that the wall pressure fluctuations can be described by following equation:

$$\mathbf{P}(k_1,k_3,\omega) = 4\rho^2 \left(\frac{k_1^2}{k_1^2+k_3^2}\right) \int_0^\infty \Lambda_2(y_2) \left[\frac{dU_1(y_2)}{dy_2}\right]^2 \cdot \tilde{\phi}_{22}(y_2,k_1,k_3) \cdot \phi_m(\omega - k_1 U_c) \cdot \left\langle u_2^2(y_2)\right\rangle \cdot e^{-2|\mathbf{k}|y_2} dy_2. \qquad (1)$$

Here Λ_2 is the integral length scale in wall normal direction. It roughly describes the vertical extension of the energy containing eddies passing the trailing edge. U_1 is the velocity of the flow at the trailing edge in streamwise direction and Φ_{22} is the spectrum of vertical velocity fluctuations. The moving axis spectrum Φ_m describes the distribution of energy away from the convective ridge (in the k_1-ω plane) for the energy in the vertical velocity and $\langle u_2^2(y_2)\rangle$ is the Reynolds stress component in wall normal direction. k_i are the wave numbers in i-direction (see also figure 1) and ω is the angular frequency.

Rnoise uses the solution of a RANS simulation obtained from the CFD codes FLOWer [6] or TAU [7], both developed by the DLR (Deutsches Zentrum für Luft und Raumfahrt). The boundary layer profile $U_1(y_2)$ is directly taken from the RANS result, but all other variables must be modelled from different boundary layer parameters, depending on the used turbulence model [4].

Finally the propagation to the farfield is calculated by solving the diffraction problem [8]:

$$S(\omega) = \frac{L}{4\pi R^2} \int_{-\infty}^{\infty} \frac{\omega}{c_0 k_1} \mathbf{P}(k_1,0,\omega) dk_1. \qquad (2)$$

Here L is the length of the trailing edge, R is the observer distance to the trailing edge and c_0 is the speed of sound.

Based on equation (1) an actuation device must be found that affects the shown parameters so that the pressure fluctuations are reduced. It is obvious that a

reduction of Λ_2, Φ_{22} and $<u_2^2(y_2)>$ will lead to reduced pressure fluctuations and subsequently to lower noise emission (eq. 2).

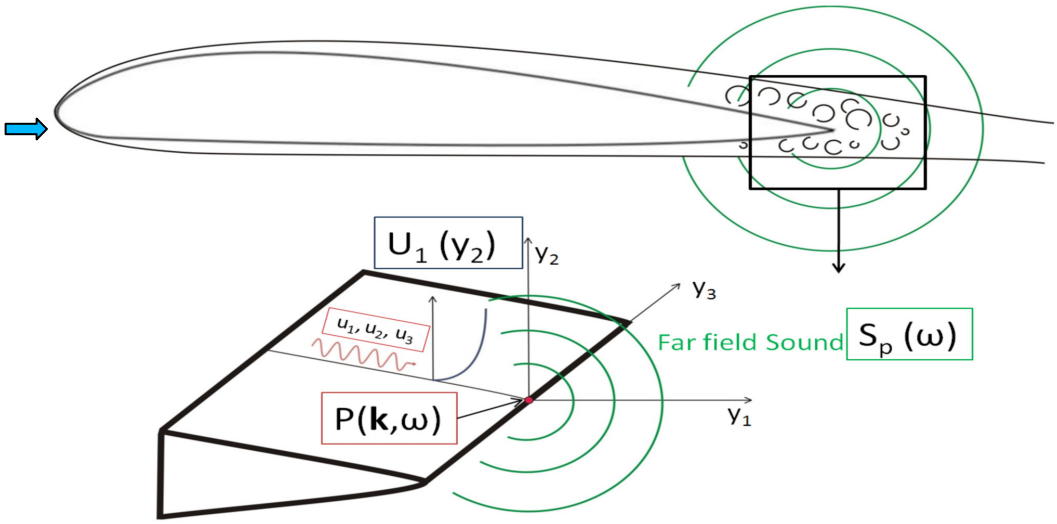

Fig 1: Schematic presentation of the production of trailing edge noise

As a first opportunity constant suction was considered to have the mentioned effects on the relevant boundary layer parameters as it is known to reduce the boundary layer thickness (and with it Λ_2) and to reduce the turbulence within the boundary layer (reduction of Φ_{22} and $<u_2^2(y_2)>$).

To give proof to this assumption, 2D CFD simulations of a NACA64-418 airfoil with a small single slot on the upper surface were performed using the TAU code. The TAU code is an unstructured finite volume code. The mesh was generated by IGG from NUMECA [13]. The y+ value which defines the height of the first cell row is set to 1. In the region of the suction slot and at the trailing edge the mesh is refined. The slot is meshed with 20 cells in streamwise direction. The simulation is fully turbulent. Figure 2 shows the solution of one of these simulations. The Mach number was set to 0.15 and the Reynolds number was 3.5e6. The magnified image on the upper left of figure 2 depicts the flow region at the actuator position. It shows how a part of the passing flow displayed by streamlines is sucked into the airfoil. In these

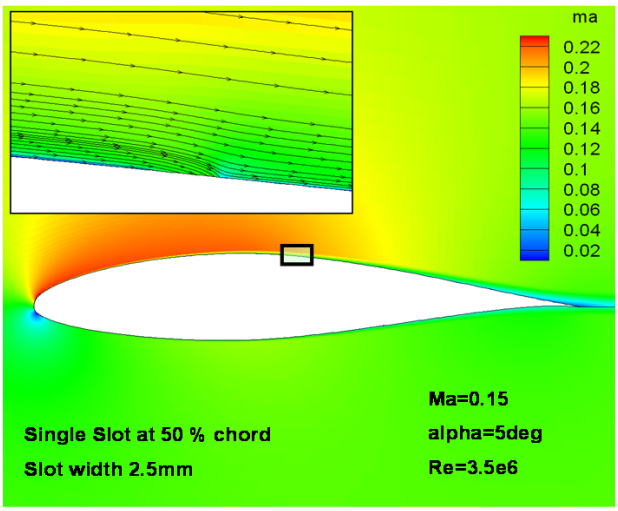

Fig 2: RANS solution of NACA64-418 with local suction slot at 50% chord. The slot width is 0.25% of chord length. The magnified picture shows the area near the slot.

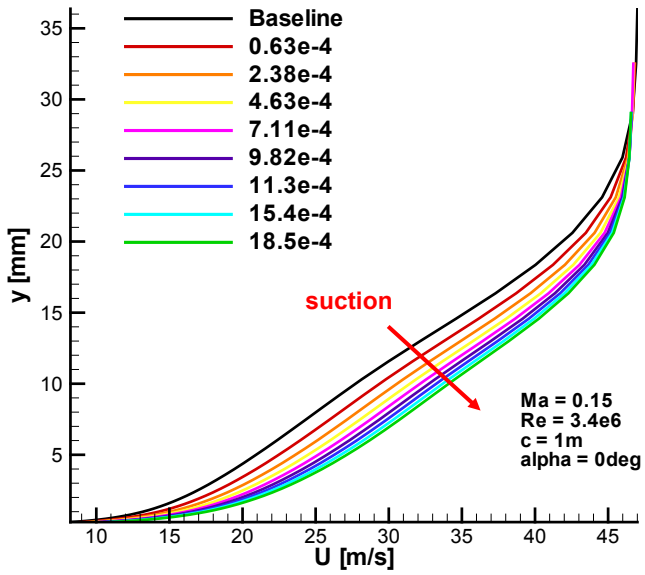

Fig 3: Velocity profile extracted directly at the trailing edge on the upper side of the NACA64-418 airfoil for the baseline and different suction rates described by momentum coefficient c_μ. Actuator positioned at 70% chord. Slot width is 0.25% of chord length.

first simulations the actuator was simulated by a pressure reservoir boundary condition defining a pressure on the surface smaller than the static pressure of the undisturbed passing flow at this position.

RANS simulation of single slot actuators were performed for different suction rates, slot widths and actuator positions. Figure 3 shows the velocity profile extracted directly at the trailing edge for different suction rates and for the baseline without suction. In these simulations the actuator was positioned at 70% chord. The suction rate is described by the momentum coefficient, which is described as

$$c_\mu = \frac{\dot{m} \cdot v_w}{1/2 \rho U_\infty^{\ 2} \cdot A_{ref}} \quad (3)$$

Here m is the massflow through the actuator, v_w is the suction velocity, U_∞ is the freestream velocity and A_{ref} is the projected surface of the airfoil. As it can be seen the velocity profile becomes fuller with increased suction rate. This causes a larger velocity gradient close to the wall. Further away from the airfoil surface the gradient is reduced. A zero gradient is reached for smaller wall distances than for the baseline indicating a smaller boundary layer thickness. A smaller boundary layer thickness leads to a smaller integral length scale Λ_2 as visible in figure 4a.

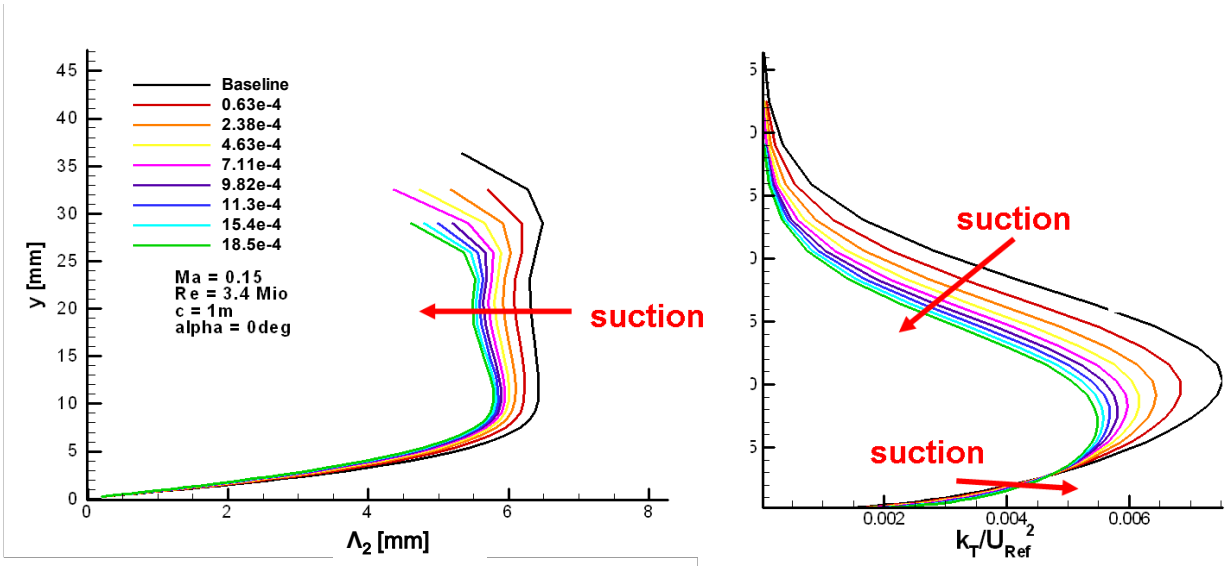

Fig 4a and 4b: Integral length scale and turbulent kinetic energy of a NACA64-418 RANS solution with local suction. Slot position: 70% chord, slot width: 0.25% chord. The legend showes the massflow coefficient c_μ. Turbulence kinetic energy normalized by $U_{Ref} = (R*T)^{0.5}$. R is the gas constant and T is the freestream temperature.

Figures 4a and 4b show the distribution of integral length scale and turbulence kinetic energy in wall normal direction. The results are again extracted directly at the upper side of the trailing edge. For the integral length scale a significant reduction can be recognized for increasing suction rate. The same effect is visible for the turbulent kinetic energy. It is used as replacement for the parameter $<u_2^2>$, introduced in equation (1). In case of isotropic turbulence it can be assumed that,

$$< u_2^2 >= \frac{2}{3} k_T \qquad (4)$$

Both effects indicate a reduction of trailing edge noise. For the turbulence kinetic energy a small increase can be seen very close to the wall. This will have a negative effect on the noise emission at high frequencies. At figure 5 the noise spectra are shown for the different suction rates evaluated by Rnoise. Clearly visible is the noise reduction at low frequencies. But at higher frequencies a noise increase is recognized. A final analysis of these spectra showed that in total a noise reduction could be achieved.

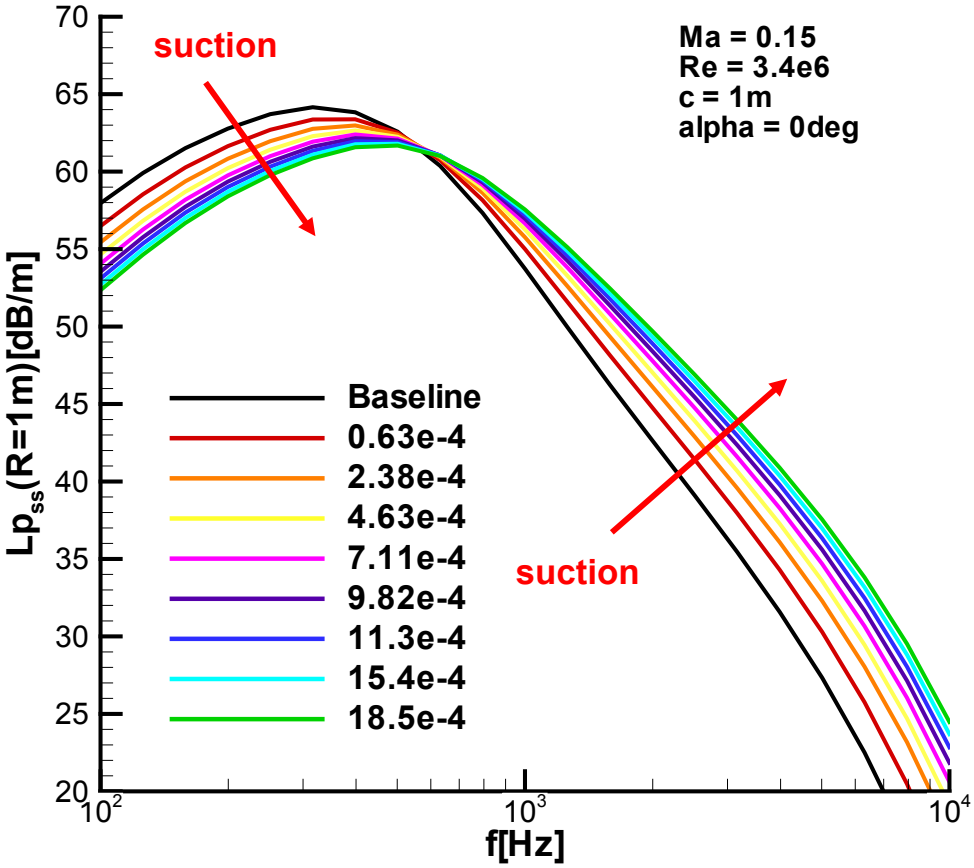

Fig 5: Noise spectra for a NACA64-418 RANS solution with local suction. Slot position: 70% chord, slot width: 0.25% chord. Suction rate is described by the massflow coefficient c_μ

Wind Tunnel Tests (Tel-Aviv)

Parallel to the simulations at the University of Stuttgart experiments investigating the effect of suction on boundary layer parameters were performed at Tel-Aviv University (TAVU). Instead of local slots the suction was applied over a large area using a porous plate. The experiments were conducted in the mixing-layer facility, located at the Meadow Aerodynamics lab at TAVU, described by Oster and Wygnanski [9]. A mixing layer facility simulates the flow conditions as they occur at the trailing edge of a cambered airfoil. The facility mainly comprises of two inflows and one plate between these inflows, as shown in figure 6.

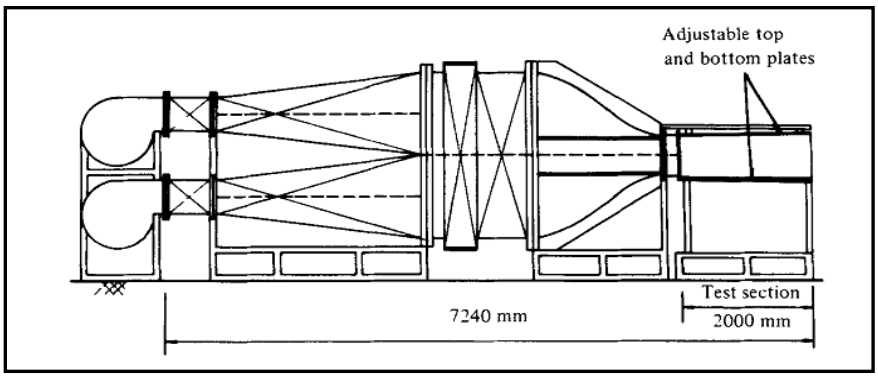

Fig 6: Mixing layer facility at Tel-Aviv University

The velocity of the slower stream (bottom test section) was 5±0.2 m/s, and the velocity of the faster stream was 7±0.2 m/s. The data was acquired with a single hot wire and a pair of X-shaped hot-wires operated at a constant temperature mode and calibrated in a manner described by Oster and Wygnanski [9]. The single hot-wire was used mainly to identify locations where the low spatial resolution of the X-wire (about 1mm) adversely affected the reliability of the data and above the splitter plate.

The airfoil aft region suction is simulated by the addition of a splitter plate to the mixing layer facility. The splitter plate suction area is 75mm long by 529mm wide. The plate porosity is 26% with suction holes diameter of 0.8mm.

A comparison between different flow features at the mixing layer region is shown in Figures 7a and 7b. The velocity profiles are turbulent. The influence of the suction technique is evident not only on higher statistics but also on the mean velocity profile.

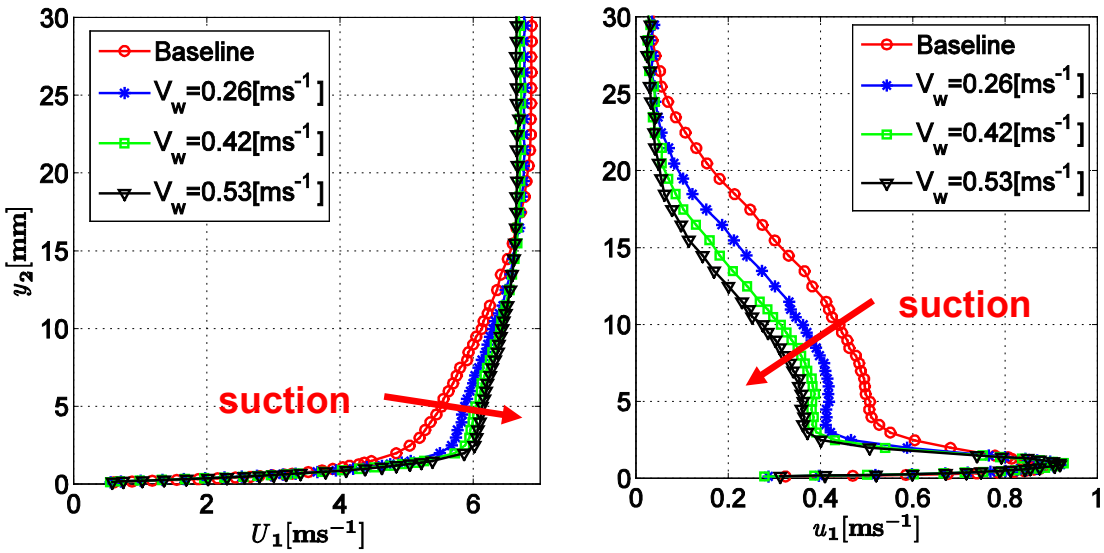

Fig 7a and 7b: Distribution of mean velocity (a) and velocity fluctuations (b) in wall normal direction for different suction velocities and the baseline configuration without suction.

Following the acquisition of the mean velocity profiles, the integral parameters of the boundary layers, with and without suction were computed (Figure 8). For the mixing layer data sets, only the upper surface ("suction" in airfoil terminology) boundary layer was taken into account. Figure 8 presents the displacement thicknesses measured upstream and downstream of the trailing edge, respectively. It is evident that by taking into account only the upper part of the boundary layer (above the wake), the influence of the boundary layer suction is evident in the data and is consistent for both measurement locations. As expected, the displacement thickness decreases with increasing suction magnitude. The same effect was discovered for the momentum thickness.

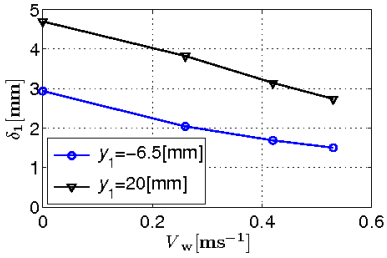

Fig 8: Effect of suction on displacement thickness measured 17.4mm upstream of the splitter plate (blue circles) and in the upper part of the wake 20mm downstream of the splitter plate (black triangles).

Figures 9a and 9b show the velocity gradient and the velocity fluctuations in wall normal direction respectively for different suction rates. Both are reduced for increasing suction velocity. Regarding equation (1) this will have a positive effect on the emitted trailing edge noise.

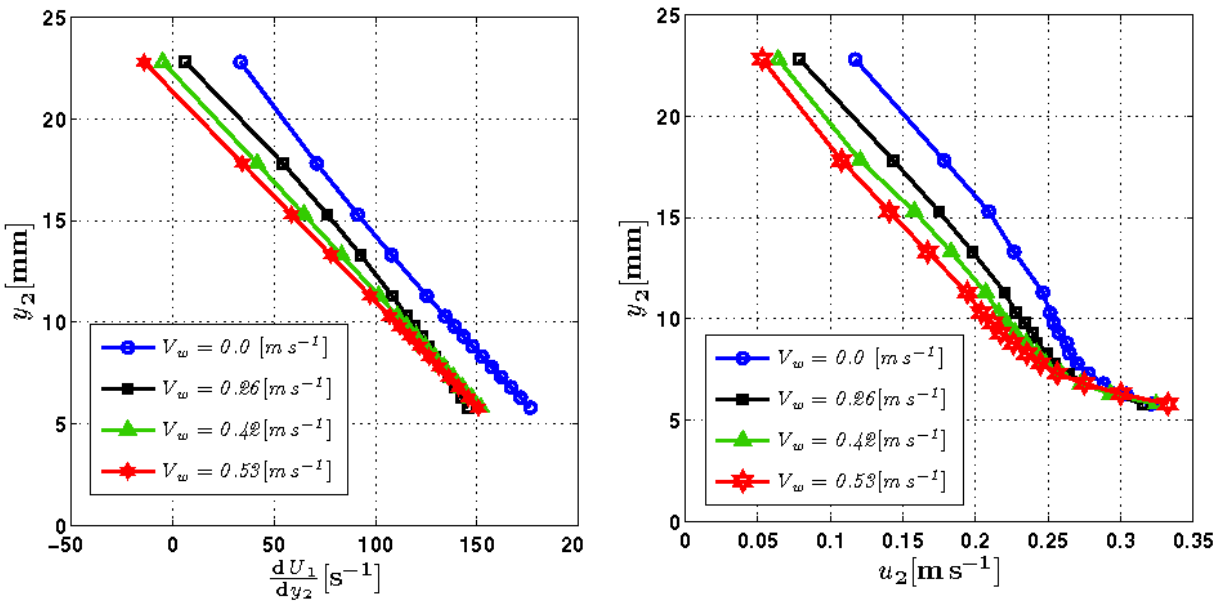

Fig. 9a and 9b: Velocity gradient (a) and velocity fluctuations in wall normal direction (b) at the trailing edge of the splitter plate.

Wind Tunnel Tests (University of Stuttgart)

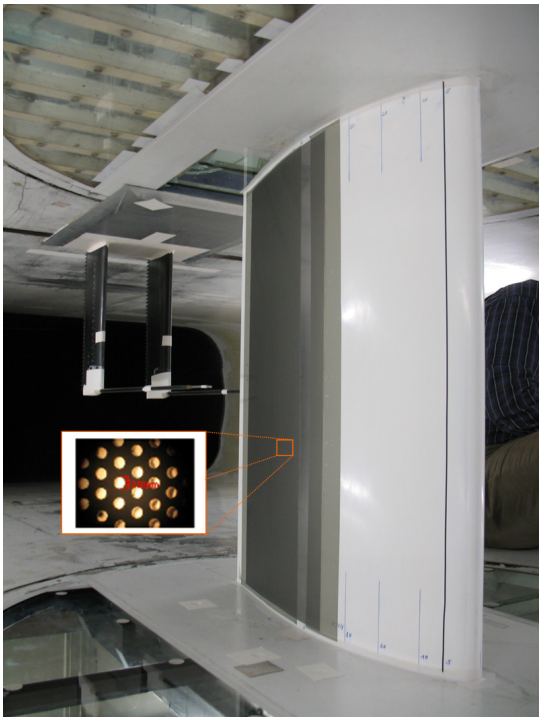

Fig. 10: Picture of the NACA64-418 inside the Laminar Wind Tunnel of the IAG with CPV-System. The magnified picture shows the holes of the porous plate. Each hole has a diameter of 250µm.

To prove the results achieved by CFD simulations and boundary layer measurements at Tel-Aviv University additional wind tunnel tests of a NACA64-418 airfoil with suction device were performed in the Laminar Wind Tunnel of the IAG [10]. The model was equipped with a distributed suction device covered with a porous plate. The holes of this plate had a diameter of 250µm and the open area was 25% of the plate area. That way suction could be applied on the upper side of the airfoil from 40 to 90 percent chord. In practice a smaller region was used to prevent circulatory flow in the actuator box caused by the streamwise pressure gradient. This could only be avoided by reducing the width of the suction area by adhesive foil and increasing the suction rate. Usually suction was applied over the whole span of the model (0.73m) and 10% of chord length. Aerodynamic and aeroacoustic measurements were performed. The latter was done by the CPV method [11]. This method developed at the Laminar Wind Tunnel was applied for trailing edge noise measurements. Special hot-wires are used for the measurement of particle velocity and the velocity fluctuations are converted to sound pressures assuming sources of monopole type located at the trailing edge. From the phase of the cross correlation function it is possible to distinguish between trailing edge noise and background noise. The hot wires are mounted on two cantilevers which have the shape of a symmetric airfoil. The trailing edges of these cantilevers are equipped with serrations to minimize the trailing edge noise emissions of the cantilevers and therefore to minimize the disturbances on the trailing noise measurements. The two cantilevers are mounted on a flat plate which is attached to the turn table. The CPV system is shown in figure 9 together with the NACA64-418 model and a magnified picture showing the holes of the porous plate. For details of the method see [11] and [12].

The results of the aeroacoustic measurements are shown in figure 10 exemplarily for an actuator position from 55% to 65% chord. Like in the CFD simulations of the single slot suction a noise reduction at low frequencies was achieved while at high frequencies a noise increase is obtained. Calculating the total noise a reduction of up to 5dB was received.

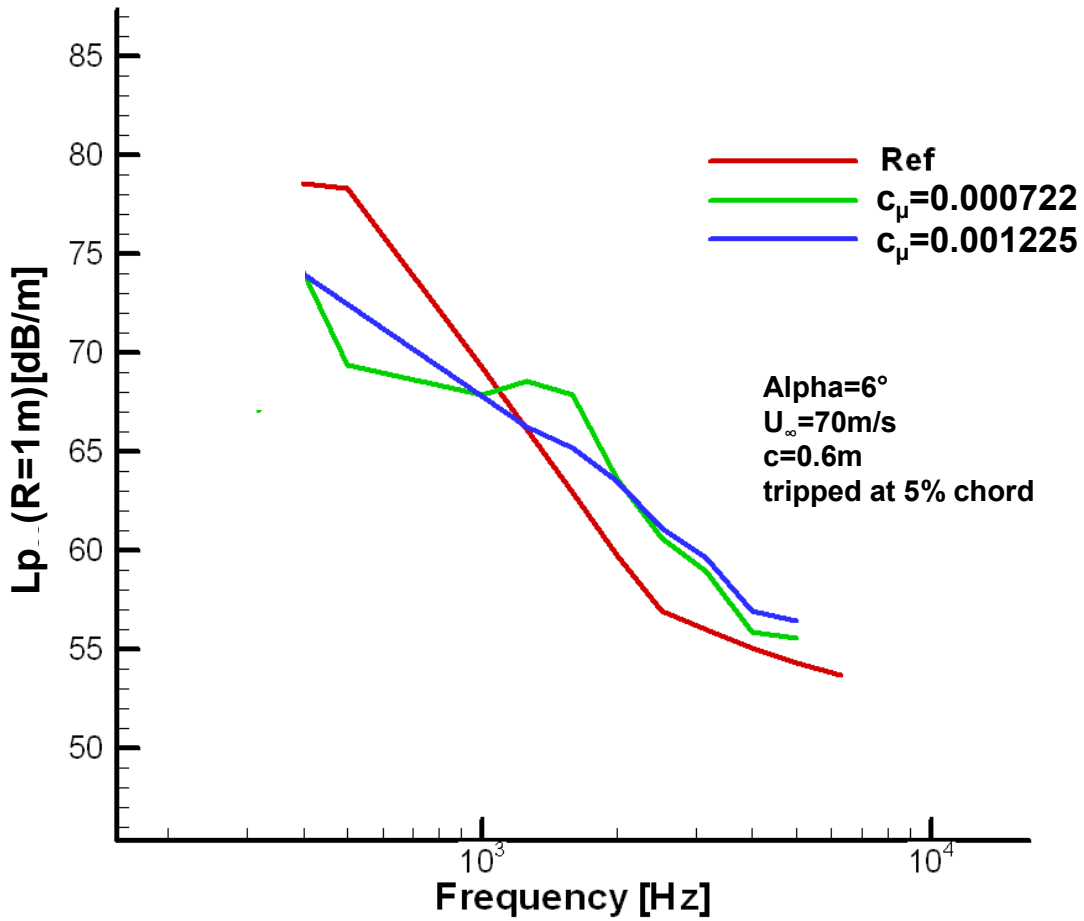

Fig 11: Measure Noise spectra of a NACA64-418 airfoil. Suction was applied from 55% to 65% chord.

Conclusions

Steady distributed suction proved as a suitable method for trailing edge noise control. CFD simulation of single slots showed the positive effect on different boundary layer parameters like length scale, turbulent kinetic energy and the velocity profile leading to a significant reduction of pressure fluctuations inside the boundary layer, which are responsible for trailing edge noise. Boundary layer measurements performed in a Mixing Layer facility by Tel-Aviv University showed in general the same characteristics, although distributed suction was applied instead of local suction. Finally aeroacoustic measurements in the Laminar Wind Tunnel of the University of Stuttgart showed that the trailing edge noise could be reduced by distributed suction by around 5dB.

References

[1] S. Oerlemans, M. Fisher, T. Maeder, K. Kögler, ”Reduction of Wind Turbine Noise using Optimized Airfoils and Trailing-Edge Serrations”, AIAA 2008-2819

[2] Th. Lutz., A. Herrig, W. Würz, M. Kamruzzaman, and E. Krämer, “Design and wind-tunnel verification of low noise airfoils for wind turbines”. AIAA 2006-3322, June 2006.

[3] M. Herr, “Design Criteria for Low Noise Trailing Edges”, DLR Braunschweig, AIAA 2007-3470

[4] M. Kamruzzaman, Th. Lutz, A. Herrig and E. Krämer, “RANS Based Prediction of Airfoil Trailing Edge Far-Field Noise: Impact of Isentropic & Anisotropic Turbulence”, AIAA 2008-2867 Paper

[5] W. Blake, “Mechanics of Flow Induced Sound and Vibrations”. Vols. 1-2 Acad. Press. New-York (1986).

[6] N. Kroll, J. K. Fassbender, “MEGAFLOW – Numerical Flow Simulation for Aircraft Design”, Springer Verlag Berlin/Heidelberg/NewYork, ISBN 3-540-24383-6

[7] J. Evans, M. Galle, T. Gerhold, “Technical Documentation of the DLR TAU-Code”, Braunschweig 2009

[8] K.I. Chandiramani. “Diffraction of evanescent wave with application to aerodynamically scattered sound and radiation from unbaffled plates.” J. Acoust. Soc. Amer., 55:19-29, 1974.

[9] S Oster, D. and Wygnanski, I., “The forced mixing layer between parallel streams”. JFM 123, 91 (1982).

[10] F. X. Wortmann and D. Althaus. ’’Der Laminarwindkanal des Instituts für Aero- und Gasdynamik an der Technischen Hochschule Stuttgart“. Zeitschrift für Flugwissenschaften, 12(4):129 134, April 1964.

[11] A. Herrig, W. Würz, Th. Lutz, and E. Krämer. “Trailing-edge noise measurements using a hotwire based coherent particle velocity method”. 24th Applied Aerodynamics Conference, San Francisco, California, 5 8 June 2006, (2006-3876), 2006.

[12] Andreas Herrig. “Validation and Application of a Hot-Wire based Method for Trailing-Edge Noise Measurements on Airfoils”. Doctoral thesis, Faculty of Aerospace Engineering and Geodesy, University of Stuttgart, 2010.